Asynchronism Induces Second Order Phase Transitions in Elementary Cellular Automata

Nazim A. Fatès

Asynchronism Induces Second Order Phase Transitions in Elementary Cellular Automata

NAZIM FATÈS*

LORIA – INRIA Nancy Grand-Est, Campus Scientifique B.P. 239
54 506 Vandoeuvre-lès-Nancy, France.

Received XXX ; In final form YYY

Cellular automata are widely used to model natural systems. Classically they are run with perfect synchrony, *i.e.*, the local rule is applied to each cell at each time step. A possible modification of the updating scheme consists in applying the rule with a fixed probability, called the synchrony rate. For some particular rules, varying the synchrony rate continuously produces a discontinuity in the behaviour of the cellular automaton. We investigate the nature of this change of behaviour using Monte-Carlo simulations. We apply a two-step protocol to show that the change of behaviour is a phase transition whose critical exponents are in good agreement with the predicted values of directed percolation and parity conservation universality classes.

Key words: asynchronous cellular automata, stochastic process, discrete dynamical systems, directed percolation, phase transitions, universality class, Monte Carlo simulations, power laws

Foreword: In this article, we only present a limited set of plots showing our numerical experimentation. The complete set of graphs can be accessed at : `http://www.loria.fr/~fates/Percolation/results.html`

* email: `Nazim.Fates@loria.fr`

1 INTRODUCTION

With the development of computing power, cellular automata (CA) are becoming a popular tool used to simulate various real-world systems. While the first research were mainly concerned the study of logical properties of abstract models [24], many efforts now focus on using CA which closely mimic natural or artificial phenomena.

Our research aims at studying the robustness to asynchronous updating of cellular automata, *i.e.*, to evaluate to which extent a small modification of their updating scheme may perturb their behaviour. To tackle this problem, we proposed to study not only a single model but a *family* of models, where the members are obtained by keeping the local rule constant and by varying the updating scheme [11]. One simple way of producing such variations is to consider the so called α-*asynchronous dynamics* [15], in which each cell independently updates its state with probability α, the *synchrony rate*, at each time step.

Such asynchronous models were studied experimentally in [13] and it was shown that the 256 elementary cellular automata (ECA) produced various qualitative responses to asynchronism. One of the most surprising phenomenon was that some rules changed their behaviour abruptly when changing slightly the synchrony rate. The present work is devoted to understanding these brutal transitions with an experimental approach. Extending the first investigations presented in [12], we show that this singular behaviour of the rules found in this class can be explained as second order phase transitions.

To our knowledge, the problem of evaluating the change of behaviour of an asynchronous CA was at first addressed in [6] by means of simulation, their evaluation of changes remaining qualitative. Other experimental studies such as [3, 31, 29] followed, showing that the update scheme was indeed a key point to study. On the theoretical side, few results have been obtained so far: the independence on the "update history" was shown undecidable in [16], existence of stationary distributions was studied in [22] and a first classification based on the convergence time was proposed in [14] and extended in [15].

In [13], it was then conjectured that this brutal variation was a phase transition that belonged to the universality class of *directed percolation* (see below). We emphasise that this hypothesis was mainly supported by the visual observation of the space-time diagrams produced near the critical point. The goal of this article is to investigate this hypothesis with large Monte-Carlo simulations.

2 FIRST OBSERVATIONS

This section introduces formal notations and presents the phenomenon with a first set of simple experiments.

2.1 Formal definitions of the model

Let a ring of n cells be indexed by $\mathcal{L} = \mathbb{Z}/n\mathbb{Z}$, a *configuration* is an assignment of a state to each element of $\mathcal{L}$, the space of configurations is $E_n = \{0,1\}^{\mathcal{L}}$. The *density* of a configuration is the ratio of cells in state 1 over the configuration size n. The *kinks density* is the ratio of the number of 01 or 10 patterns over the size of the configuration n. An *elementary cellular automaton* (ECA) is described by a function $f : \{0,1\}^3 \to \{0,1\}$ called the *local rule*. ECA are indexed according to Wolfram's usual notation.

We define the α*-asynchronous updating scheme* as the operation that consists in considering each cell independently and applying the local rule f with a probability α or keeping the same state with a probability $1-\alpha$. This updating scheme defines a probabilistic global rule F which operates on the random variables $(x^t)_{t\in\mathbb{N}}$ according to $x^{t+1} = F(x^t)$ such that:

$$\forall i \in \mathcal{L},\ x_i^{t+1} = \begin{cases} f(x_{i-1}^t, x_i^t, x_{i+1}^t) & \text{with probability } \alpha \\ x_i^t & \text{with probability } 1-\alpha \end{cases}$$

By taking $\alpha = 1$, we fall back on the classical synchronous case and as α is decreased, the update rule becomes more asynchronous while the effect of an update remains unchanged. For $\alpha < 1$, x^t is a random variable that depends on the *sequence of updates*, *i.e.*, the sequence of cells that are updated at each time step.

2.2 Selecting the Rules to Study

From [13], some rules were experimentally detected as showing a brutal change of behaviour when α was varied. We investigated this change of behaviour for the 88 Minimal Representative ECA rules. For each rule, we arbitrarily fixed the ring size to $n = 10\,000$ and we varied α with an increments of 1% from 0.02 to 1. For each α, we started from a uniform random initial configuration and we measured the evolution of the density during $10\,000/\alpha$ steps, putting a limit to $100\,000$ steps for $\alpha < 0.1$. The average was computed on the second half of the sample, the first half being used as a transient period, to ensure that the system was stabilised. This average density can be considered as an approximation of the *stationary density*, *i.e.*, the limit density that would be reached for a system size and a transient time growing to infinity.

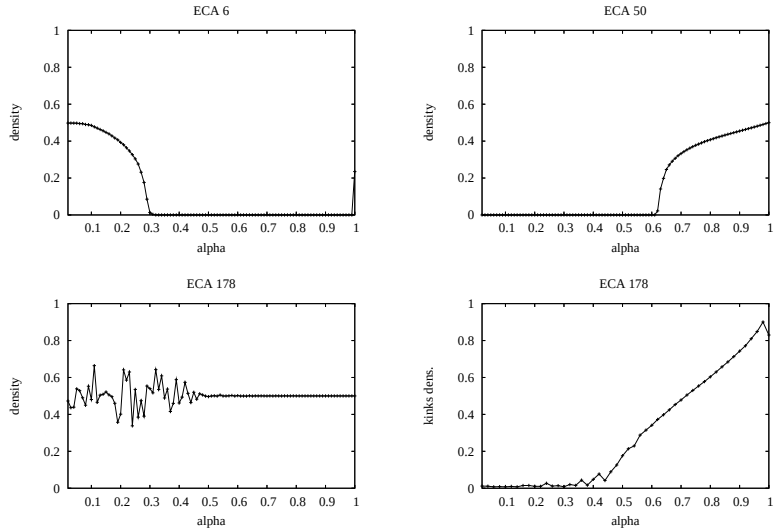

FIGURE 1
(top) Stationary density versus synchrony rate for ECA 6 (left) and ECA 50 (right). (bottom) ECA 178 : stationary density (left) and kinks density (right) versus synchrony rate. The discontinuity for ECA 6 and 178 at $\alpha = 1$ is not an artifact.

Figure 1 shows how this measure varies with α for ECA 6, 50, and 178. We observed that, among the 88 rules examined, ECA 18, 26, 58, 106, 146 all have plots which are similar to ECA 50. As we believe that this behaviour is due to *directed percolation* (see later), with an active phase obtained for *high* values of α, we call these rules the $\mathsf{DP}_{\mathrm{hi}}$ ECA. Their behaviour is compatible with a second order phase transition: there exists a critical value of α such that for $\alpha > \alpha_{\mathrm{c}}$, the stationary density is non-zero (the *active* phase) and for $\alpha < \alpha_{\mathrm{c}}$ the stationary density is zero (the *inactive* phase). The curve is continuous and reaches zero with an infinite slope for the critical value α_c. ECA 6, 38 and 134 displayed a similar behaviour but their phase-transition was found in an "inversed" pattern: the active phase is obtained for *small* values of α, the inactive phase for large values of α. We call these rules the $\mathsf{DP}_{\mathrm{lo}}$ ECA.

The case of ECA 178 is peculiar since the density curve is stable for large values of α but does not converge to a stable value for small values of α. This

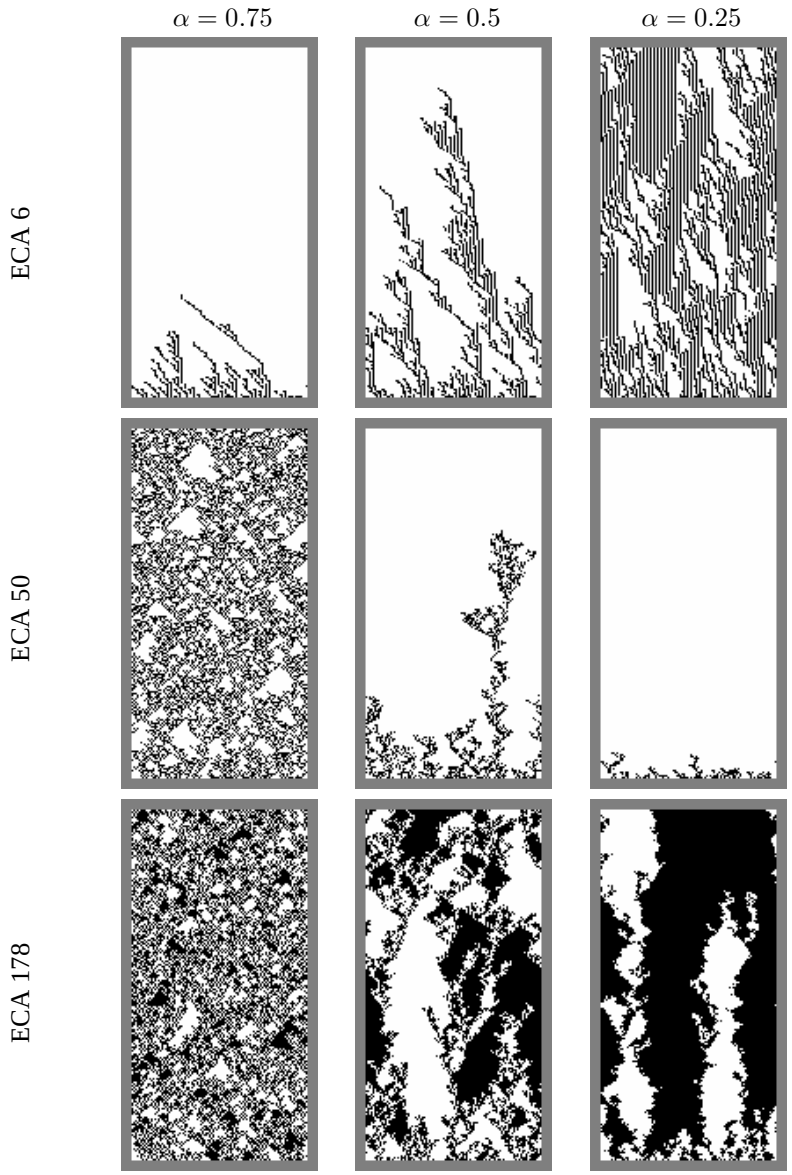

FIGURE 2
Space time diagrams for ECA 6 (top), ECA 50 (middle) and ECA 178 (bottom). Synchrony rate varied : $\alpha = 0.75$ (left), $\alpha = 0.50$ (middle), $\alpha = 0.25$ (right). Time goes from bottom to top; the time factor is rescaled by a factor $1/\alpha$ (i.e., for $\alpha = 0.25$ only time steps that are multiples of 4 are displayed).

indicates that for this particular rule, the choice of measuring density is not suitable. Instead, if we examine the variation of the *kinks* density, we obtain a smooth curve with a discontinuity compatible with a second order phase transition. We call this rule the DP_2 ECA (the choice of this name is justified later).

Figure 2 shows how the variation of synchrony rate affects the space-time diagrams of rules 6 ($\mathsf{DP}_{\mathrm{lo}}$), 50 ($\mathsf{DP}_{\mathrm{hi}}$) and 178 ($\mathsf{DP}_2$). We can divide the space-time diagrams into two categories: (a) a behaviour with stable branching-annihilating patterns, observed for the active phase ; (b) a behaviour where the branching-annihilating patterns tend to disappear, observed for the inactive phase.

3 PHASE TRANSITIONS

In this section, we present a short review of other works related to asynchronous or probabilistic cellular automata and second order phase transitions.

3.1 Universality classes

Many physical or numerical systems exhibit critical phenomena: a continuous change in the value of a control parameter may produce a discontinuous answer at the macroscopic level. It is remarkable that near the critical transition, the laws governing the evolution of such systems are generally power-laws. Intuitively, one may understand the origin of these power-laws from the fact that near the transition point, the system has a self-similar fractal structure and thus no typical spatial wavelength. An important property is that the same exponents of the power laws, the *critical exponents*, may be found for different models.

The collection of all phenomena that are described by the same set of critical exponents is called a *universality class*. Looking at the space-time diagrams produced by the asynchronous ECA, we originally found similarities with the patterns produced by couple map lattices used in hydrodynamics [1]. These similarities lead us to identify our phase transition as possibly belonging to the *directed percolation* (DP) universality class.

It is out of scope to list all the phenomena that belong to the directed percolation universality class and we refer to [18, 28] for a review. As far as cellular automata are concerned, directed percolation was observed in various problems. To our knowledge, the first CA that was shown to exhibit DP is

the Domany-Kinzel cellular automaton [21, 8]. This model is a tunable probabilistic CA that has the ability to display two different transitions depending on the values of its parameters. Various other models involving probabilistic CA were also shown to exhibit DP phenomena (*e.g.*, [26, 27]).

Directed percolation was also identified in problems involving synchronisation of two copies of cellular automata (*e.g.*, [17, 30]). To our knowledge, the only example of directed percolation induced by asynchronism was given by Blok and Bergersen for the famous Game of Life [4]. The protocol they used to identify the universality class of the phase transition relied on the measure of a single critical exponent, the β exponent (see below).

3.2 Phase transitions and universality classes

Percolation problems are studied in the fields of discrete mathematics and statistical physics. They were initially motivated by the need to model situations in which a fluid has to evolve into a porous random medium [5]. In the classical problem of *isotropic percolation*, the porous medium is modelled by a regular infinite two-dimensional square lattice. The nodes of the lattice, or *sites*, can be either *open* (with probability p) or *closed* (with probability $1-p$) ; the links between the sites, or *bonds* can also be either *open* (with probability q) or *closed* (with probability $1-q$). Starting from an initial set of *wet* sites, the question is to determine the set of sites that will also be *wet* if the liquid flows into open sites and open bonds. The sets of all wet sites connected through closed bonds and sites is called a *cluster*.

If we set $p=1$ (respectively $q=1$), we have the isotropic *bond* (resp. *site*) *percolation*. For the isotropic bond percolation problem, the average cluster size diverges for the critical value $p_c = 1/2$.

Directed bond percolation is as a non-isotropic variant of the previous model in which links are oriented according to a particular direction. It models situations in which the fluid can go only in one direction, *e.g.*, when submitted to gravity. Directed percolation can also be formulated in terms of a probabilistic dynamical system: in this case, time plays the role of the non-isotropic dimension. More formally, if the state of a site $i \in \mathbb{N}$ at time t is represented by $s_i^t \in \{0,1\}$ (dry or wet site), starting from an initial condition s^0, the states of sites are updated according to the simple rule [18]:

$$s_i^{t+1} = \begin{cases} 1 & \text{if } [s_{i-1}^t = 1 \text{ and } \mathcal{L}_i^t(p) = 1] \text{ or } [s_{i+1}^t = 1 \text{ and } \mathcal{R}_i^t(p) = 1] \\ 0 & \text{otherwise} \end{cases}$$

where $(\mathcal{L}_i^t)$ and $(\mathcal{R}_i^t)$ are i.i.d. Bernoulli random variables ; they model the probability for the left or right bound to cell (i,t) to be opened or closed (see

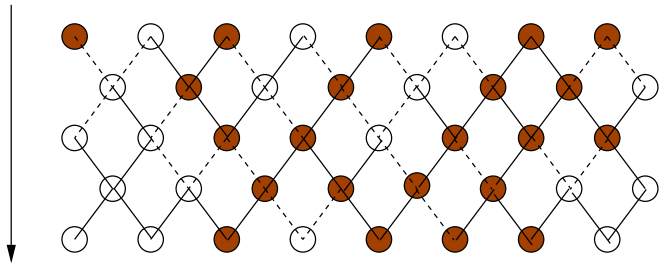

FIGURE 3
Example of directed bond percolation: filled circles are wet sites, empty circles represent dry sites ; solid (resp. dashed) represent open (resp. closed) bounds.

Figure 3 for an illustration).

Theory and observations [18] predict that for an *infinite* lattice and for a fixed value of p, if we start from an initial configuration with all sites in wet state, the density of wet sites $d(p,t)$ evolves to a positive limit for $p > p_c$ and to a zero limit for $p \leq p_c$. More precisely, if we denote by $d_\infty(p)$ the infinite time limit of $d(p,t)$, for $p > p_c$, near the critical point ($p \to p_c$), the asymptotic density d_∞ diverges from zero by following a power law:

$$d_\infty(p) \sim (p - p_c)^\beta$$

Note that as we have $\beta < 1$, the right derivative of $d_\infty(p)$ has an infinite value at the critical point. At the critical point $p = p_c$, the density vanishes to zero $d_\infty(p_c) = 0$ and the decrease follows a power law:

$$d(p_c, t) \sim t^{-\delta}$$

The values of the two critical exponents $\delta = 0.1595$ and $\beta = 0.2765$ are known by numerical simulations (the values are given here with four digits, see [18] for a better precision). It is so far an open problem to determine whether these exponents are rational numbers or not. There are also other critical exponents that can be used to identify a universality class but we here choose to focus only on the measure of β and δ exponents (following [25, 17] for instance).

3.3 The PC-DP2 class

In the case where the local rule has two *symmetric* absorbing cases, it is generally observed that the phase transition is in one of the two universality classes: either the $\mathbb{Z}_2$-*symmetric directed percolation* (DP_2) class or the *parity-conserving* class (PC). Again, we refer to [18, 28] for a detailed description of these two universality classes, their similarities and differences. In short, we indicate that the PC universality class appears when one considers models with branching-annihilating random walks with an *even* number of offspring (*e.g.*, [20]). The DP_2 class is observed with models that introduce two *symmetric* states, as it is the case for ECA 178.

It is well known that the two classes coincide for dimension 1 and differ for higher dimensions. An intuitive reason for this surprising property is indicated by Hinrichsen [18] : "active sites of PC models in $d \geq 2$ dimensions can be considered as branching-annihilating *walkers*, whereas DP_2 models describe the dynamics of branching annihilating *interfaces* between oppositely oriented inactive domains". From the observation of space-time diagrams of ECA 178 distinction, we conjectured in [11] that the phase transition of this rule belonged to the DP_2 universality class.

3.4 Hypotheses to test

The phase transition theory stipulates that there should be two macroscopic parameters, respectively called *the control parameter* and *the order parameter*, that satisfy the power laws of DP when the control parameter is varied. For the sake of simplicity, we propose here to use the synchrony rate α as a control parameter and the density d as an order parameter. However, note that other possibilities may also be examined, for example in [4] the authors also use the *activity* (*i.e.*, the ratio of cells in an unstable state) as an order parameter. For the nine DP ECA, we thus expect to measure:

- $d(\alpha_{\mathrm{c}}, t) \sim t^{-\delta}$ at the critical point.
- $d_\infty(\alpha) \sim {\Delta_\alpha}^\beta$ near the critical point, for the active phase,

with $\Delta_\alpha = \alpha - \alpha_{\mathrm{c}}$ for the $\mathsf{DP}_{\mathrm{hi}}$ ECA and $\Delta_\alpha = \alpha_{\mathrm{c}} - \alpha$ for the $\mathsf{DP}_{\mathrm{lo}}$ ECA. For ECA 178, we take the kinks density as an order parameter. By contrast with the DP universality class the exponents of the DP_2 class are known analytically. In particular we have $\delta_{\mathrm{DP2}} = 2/7$ for one-dimensional lattices.

3.5 Protocol and Measures

The measure of the DP critical exponents is a delicate operation that generally requires large amount of computation time. The main difficulty resides

in avoiding systematic errors when obtaining statistical data near the transition point. It happened that authors were mislead by their measures and concluded that a phase transition phenomenon was not in the DP universality class, which was later proved wrong by using a different protocol and more precise measures [19, 17]. In order to limit the influence of systematic errors, we take the two-step protocol used in ref. [17]:

- We measure the critical synchrony rate α_c by varying α until we reach the best approximation of a power-law decay for the density. This first experiment also allows us to measure the critical exponent δ.
- We measure the stationary density d_∞ as a function of $|\alpha - \alpha_c|$ and then fit a power-law in order to calculate β.

Note that these two steps are not independent since the second operation uses the previously computed value of α_c.

Other difficulties are due to finite size effects and metastability effects. Indeed, in the active phase, finite DP systems are in an *out of equilibrium* state. This means that although infinite-size systems have a stable probability measure for the distribution of states, the finite-size systems used in the simulations may attain the absorbing state even if they are in the active phase. There exists many techniques to handle this problem, for example adding a small noise to prevent the system from reaching the absorbing state. In this work, we choose to use large size lattices and verify experimentally that the results are not influenced by the trajectories that touch the absorbing state (here $0^{\mathcal{L}}$).

We will present the curves for ECA 50 while only numerical data will be given for the others DP ECA. Indeed, rule 50 can be written in the rather simple form:

$$\forall (a,b,c) \in \{0,1\}^3,\ f(a,b,c) = \begin{cases} 1-b & \text{if } (a,b,c) \neq (0,0,0) \\ 0 & \text{if } (a,b,c) = (0,0,0) \end{cases}$$

It is possible to see this rule as a one dimensional version of an "epidemic" rule: a healthy cell (state 0) gets infected (state 1) if at least one of its neighbour is infected ; once it is infected, it becomes healthy at the next update of the cell.

All the runs will start from a uniform random configuration of size n and the sequence of updates will be varied, using the `Ranmar` random number generator (period $\sim 10^{43}$) implemented on the `FiatLux` cellular automata simulator [9].

4 FINDING THE CRITICAL SYNCHRONY RATE $\alpha_{\mathbf{C}}$

Recall that in the case of directed percolation, the critical point is determined by a change of convexity in a log-log plot. The concave function characterises the *active* phase as the asymptotic density evolves towards a non-zero value ; the convex function corresponds to the *inactive* phase as the density evolves to zero with an exponential decay.

For ECA 50, the previous experiment (Figure 1) allowed us to locate the critical synchrony rate around $\alpha_c \sim 0.62$. Figure 4 shows the temporal decay of the density as α is varied by increments of 10^{-3} around 0.62 . The change of convexity is found between 0.627 and 0.629. The curves are obtained by averaging the data on $N_{\rm s} = 100$ runs obtained on a ring size $n = 20\,000$ steps and a sampling time $T = 200\,000$.

To improve our estimate of α_c to a precision of 10^{-4}, we repeated the previous experiment, extending the sampling time to $T = 10^7$ and the ring size to $n = 40\,000$. Figure 4 shows the two $\alpha_{\rm c}^- = 0.6381$ and $\alpha_{\rm c}^+ = 0.6383$ for which we observed the change of convexity. We repeated the same type of progressive approximations of α_c for all the DP ECA. It was always possible to observe the change of convexity when varying alpha with an increment of 10^{-4}. However, the sampling time T , the ring size n and the number of samples $N_{\rm s}$ had to be adapted to each ECA to ensure a good stability of the measures (see below). The values of the critical synchrony rates are reported in Table 1.

4.1 Measurement of δ

We report in Table 1 the time interval $[T_{\rm min}, T_{\rm max}]$ used to compute δ. The lower limit $T_{\rm min}$ is obtained by a rough estimation of the maximum transient time needed for the system to enter into the power-law regime. The upper limit of the interval $T_{\rm max}$ corresponds to the minimum time for which the deviation from a power-law decay becomes visible for the curves $\alpha_{\rm c}^-$ and $\alpha_{\rm c}^+$ that show the change of convexity.

We call the reader's attention on the fact that it is a difficult problem to estimate the error on δ. Indeed, besides the influence of noise, the value depends on the time interval $[T_{\rm min}, T_{\rm max}]$ used to perform the fit. There is to our knowledge no general method for choosing this time interval. To estimate the error on δ, we computed the different values obtained when varying α to $\alpha_{\rm c}^-$ and $\alpha_{\rm c}^+$ and by varying $T_{\rm min}$ and $T_{\rm max}$ by a factor 2. Numerical estimations of δ are reported in Table 1 for comparison with $\delta_{\rm DP}$. Given our estimations of uncertainty, we observe that results show good agreement with $\delta_{\rm DP} = 0.1595$.

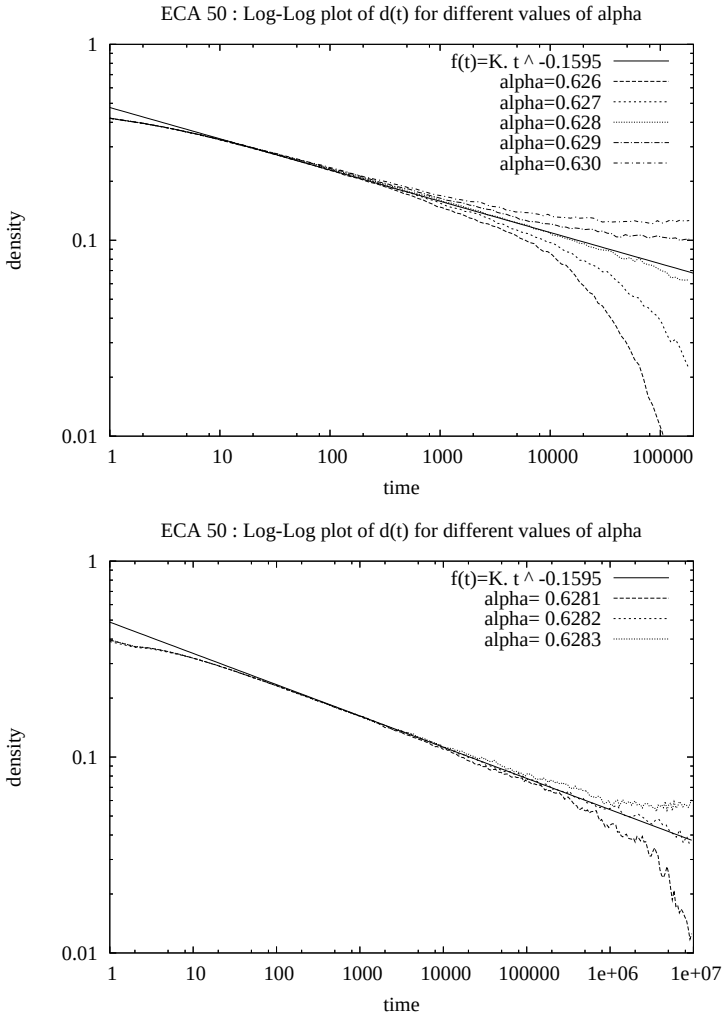

FIGURE 4
ECA 50: Determination of the critical synchrony rate α_c. (above) Averages obtained on $N_s = 100$ runs, ring size $n = 20\,000$, maximum time $T = 2 \times 10^5$. (below) Averages obtained on $N_s = 50$ runs and ring size $n = 40\,000$, maximum time $T = 10^7$. The straight line has slope $-\delta_{DP} = -0.1595$ and is plotted for reference.

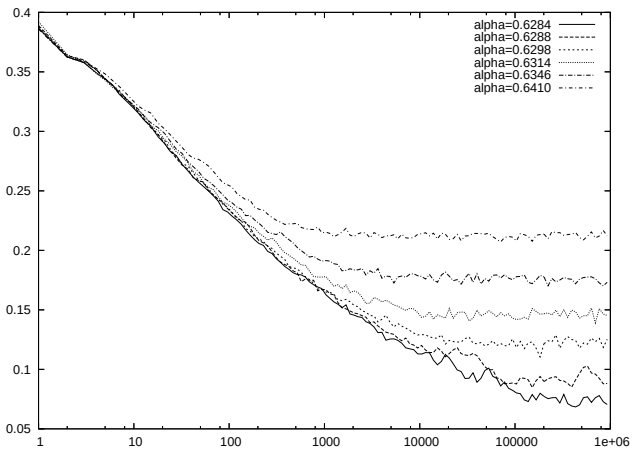

FIGURE 5
ECA 50: Evolution of the density vs. time for $\alpha > \alpha_{\rm c}$, ring size $n = 2 \times 10^4$, averaged on $N_{\rm s} = 10$ runs, with sampling time $T = 10^6$.

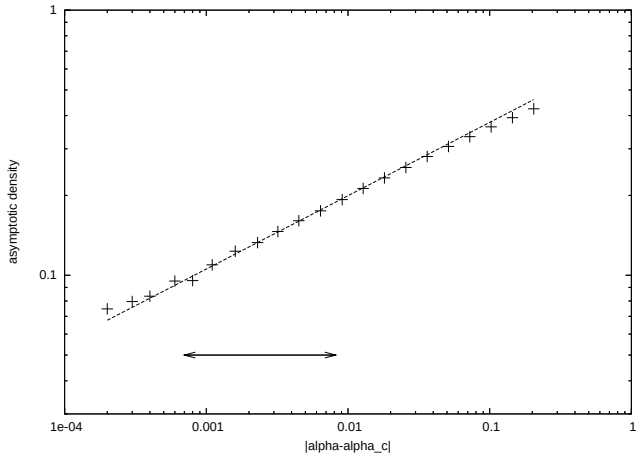

FIGURE 6
ECA 50: Determination of the critical exponent β using the time decay properties (see text). The straight line shows theoretical prediction and has slope: $\beta_{\rm DP} = 0.2765$. Note that both x and y axis are displayed in logarithmic scale. The arrow shows the fit interval used to calculate the β exponents.

4.2 Stability of the measure

For each set of measures, the change of convexity of the curves was determined both visually and numerically. A simple numerical method to estimate how linear is a curve (in a log-log representation) consists in using the root mean square error of the fit. For example, for ECA 50, fitting a power-law in the time interval $[300, 10^6]$ for $\alpha_c^- = 0.6181$, $\alpha_c = 0.6282$, $\alpha_c^+ = 0.6283$ gives an error of 0.17, 0.11, 0.15, respectively, which confirms that the "most linear" curve is obtained with α_c.

The measure of δ is more delicate since we need to distinguish three parts in the evolution of the density: the "transient" part $[0, T_{\min}[$, the "power-law" part $[T_{\min}, T_{\max}]$ and the departure from power law $[T_{\max}, \infty[$, which can be convex or concave.

Firstly, let us note that the length of transient time interval $[0, T_{\min}]$ only depends on the ECA considered while the length of the "power-law" part of the curve $[T_{\min}, T_{\max}]$ is a function of $|\alpha - \alpha_c|$, the distance to the critical point: the smaller this value, the longer the system will follow the power-law predictions. This means that the values of $T_{\max}$ heavily depend on our choice of increment on α (here 10^{-4}).

Secondly, we also need to recall that the system is in a metastable state. This implies that, whatever the value of α, the density will eventually reach the absorbing state $0^{\mathcal{L}}$. To control that our results were not influenced by the trajectories that touched the absorbing state, we followed the proportion of runs which have reached the fixed point $0^{\mathcal{L}}$. For all the DP ECA but ECA 18, we used $n = 40\,000$; for ECA 18, it was necessary to go until $n = 80\,000$ to ensure the independence of the measures with respect to the ring size n. The case of ECA 134 also needs to be underlined : its "linear" part is quite short and its "transient" part is peculiar as its density curve has many inflexion points.

5 DETERMINATION OF β

The second part of the experiments consists in measuring the β critical exponent using the values of the stationary density as a function of α. Recall that, as α approaches α_c, the stationary density vanishes as: $d_\infty(\alpha) \sim {\Delta_\alpha}^\beta$.

To estimate this stationary density, it is necessary to adjust the sampling time as a function of Δ_α. Indeed, as Δ_α approaches zero, d_∞ approaches zero and the time needed to reach this density increases exponentially with $1/\Delta_\alpha$. This phenomenon, known as *critical slowing down* (*e.g.*, [18]), limits the precision on the measure of the stationary density d_∞.

TABLE 1
Numerical Results for the DP and DP_2 critical exponents : the digit between parentheses is uncertainty on the last digit.

ECA	$\tilde{\alpha}_c$	δ	$T_{\min}$	$T_{\max}$	β
6 - BFGH	0.2825 (1)	0.160 (4)	1×10^3	2.5×10^5	0.27 (1)
18 - BCEFGH	0.71385 (5)	0.157 (3)	5×10^1	2×10^4	0.27 (1)
26 - BCEGH	0.47485 (5)	0.159 (1)	1×10^3	2×10^5	0.27 (1)
38 - BDFG	0.04085 (5)	0.159 (2)	2×10^4	3.5×10^5	0.28 (1)
50 - BCDEFGH	0.6282 (1)	0.159 (8)	3×10^2	1.5×10^5	0.27 (1)
58 - BCDEGH	0.3398 (1)	0.161 (4)	1×10^3	1×10^5	0.27 (2)
106 - BDEH	0.8146 (1)	0.157 (2)	5×10^2	3.5×10^5	0.27 (1)
134 - BFG	0.0821 (2)	0.162 (6)	2×10^4	2×10^6	0.25 (3)
146 - BCEFG	0.67505 (5)	0.158 (3)	5×10^1	1×10^5	0.28 (2)
178 - BCDEFG	0.410 (1)	0.286 (4)	1×10^2	2×10^5	? (?)

5.1 Measurement of β

In this experiment, we obtained an approximation of the stationary density $d_\infty(\alpha)$ by measuring $d(t)$ during a time $T = 10^6$ and by taking the average of d on the time interval $[T/2, T]$. To limit the influence of the noise, we repeated $N_s = 10$ times the measure and took the average value.

There are two different possibilities for varying Δ_α, some authors use linear variation (*e.g.*, [4]) while others use an exponential variation. As we expect the curve d_∞ vs. Δ_α to be linear in a log-log plot, we took an exponential increment, which allows us to obtain equally spaced points in the log-log scale. We varied $\Delta_\alpha = |\alpha - \alpha_c|$ according to an exponential increment of $\sqrt{2}$ from 8×10^{-4} to 0.512. Figure 5 shows the evolution of the density as a function of time for different values of synchrony rate.

The time interval was set independently of α. Ideally, it would be more efficient to adjust the sampling time as a function of Δ_α but at this time, we do not know how to make this adjustment. Figure 6 shows the approximated values of d_∞ as a function of Δ_α. The visual comparison with the expected plot shows a good agreement with the predicted value. For each ECA, we took $[20 \times 10^{-4}, 20 \times 10^{-3}]$ as a fit interval. The other calculated values of β are reported in Table 1. As for the δ exponent, the computed values show good agreement with the DP prediction $\beta_{DP} \sim 0.276$..

5.2 Stability of the measure

We observe that the linear part of the curves is limited by two competing phenomena. On the one hand, the small values of Δ_α are overestimated because of the critical slowing down (waiting longer means decreasing the value). On the other hand, for the higher values of Δ_α, the system "saturates" and no longer follows a power-law. The deviation from the power law is a phenomenon that is predicted by theory and that can be studied for its own interest. We prefer here to restrict our measures to the linear part of the curve. However, some authors advocate that the study of the deviations from the power law gives a power of discrimination that significantly improves the determination of a universality class [23].

To estimate the error on β, we measured how its value changed when α_c was varied in the interval $[\alpha_c^-, \alpha_c^+]$ and when the fit interval was changed to $[40 \times 10^{-4}, 40 \times 10^{-3}]$. We noticed that the error was mainly due to the uncertainty on α_c. As the value of the error was generally higher than 10^{-2}, we preferred to give β with a precision 10^{-2} rather than 10^{-3}.

6 THE CASE OF ECA 178

We repeated the same methodology as described above on ECA 178. For $n = 80\,000$; we located a change of convexity between $\alpha_c^- = 0.409$ and $\alpha_c^+ = 0.411$. However, by contrast with the previous DP ECA, this change of convexity was much more difficult to observe. It explains why we could not measure α_c with a better precision. This well-known phenomenon is explained by the algebraic decay of the kinks density in the inactive phase : it is less easy to distinguish it from the power-law than the exponential decay observed for the previous DP ECA.

In the time interval $[100, 20\,000]$, the fit for the curve $\alpha = 0.410$ gives as slope $\delta = 0.2860$, which is close to the predicted value $\delta_{\mathrm{DP2}} \sim 0.2856$.

To estimate the error on this measure, we repeated the fit with the same interval, but with α_c^+ and α_c^-. We found that δ varied less than 4×10^{-3}. As the precision on δ is satisfying while the precision on α_c is relatively poor for this rule, we did not measure the critical exponent β. A possible way of improving our measure of the critical point α_c consists in using a different experimental protocol, for example measuring other critical exponents such as the "dynamical" exponents which are obtained by starting with an initial condition close to the absorbing state.

7 DISCUSSION

The problem of determining how changes of behaviour were triggered by gradual changes in the synchrony rate were investigated by numerical simulations. The results show good evidence that the brutal change of behaviour is a second order phase transition which belongs to the directed percolation universality classes (DP and DP_2).

The observation of the synchronous behaviour of the rules studied indicate that there is certainly no straightforward relation with the existing classifications. For example, ECA 50 is "periodic" (or Wolfram class II) while ECA 18 is "chaotic" (or Wolfram class III). This indicates that near a critical point, asynchronous updating may render the details irrelevant at the microscopic cell-scale while the system is still governed globally by the same global laws. This also indicates that the observation of the asynchronous behaviour of a cellular automaton may unveil other types of complexity.

7.1 The Directed Percolation Conjecture

These results may also be discussed in the light of a famous conjecture by Janssen and Grassberger (*e.g.*, see [18] for a short presentation) that states that a model should belong to the DP universality class *if* it satisfies the following criteria: **(a)** the model displays a continuous phase transition from a fluctuating active phase into a unique absorbing state, **(b)** the possibility to characterise the phase transition by a positive one-component order parameter, **(c)** the definition of dynamics by short-range process, **(d)** and the absence of additional symmetries or quenched randomness (*i.e.*, fixed topological modifications).

For all the DP ECA, condition **(a)** is fulfilled with $0^{\mathcal{L}}$ as the absorbing state. Note that the configuration $0^{\mathcal{L}}$ a fixed point for all the rules, but ECA 134 and 146 also have $1^{\mathcal{L}}$ as a fixed point. This confirms that the informal notion of "absorbing state" can not be trivially identified with the fixed point mathematical property. Condition **(b)** was fulfilled by the density or by the kinks density. Condition **(c)** is true by definition of cellular automata. Analysing condition **(d)** is interesting since we see a difference between *space* symmetry, which is by rule 50 for example , 146, and *state* symmetry (*i.e.*, invariance under 0 and 1 exchanging), which is absent for all the DP ECA. It may also explain why rule 178, which has both symmetries, has a peculiar behaviour and was found in the DP_2 universality class.

The conditions **(b)**, **(c)**, **(d)** can be easily verified. One of the most challenging question now consists in explaining why only one small part of the 256 ECA also verify condition **(a)** and thus exhibit DP behaviour.

7.2 Perspectives

From a practical point of view, the main limitation we faced was the huge amount of computation time needed to find the critical exponents : for each rule, we used approximately 10^{15} computations of the local rule in order to be able to determine these exponents with two or three digits. This task represented several months of calculus with several personal computers. It calls further studies on how to optimise the computation process (*e.g.,* the generation of random numbers) and on how to take advantage of massively parallel computing devices such as Graphical Processor Units.

At this point, it appears that it is still an intriguing question to understand the origin of out of equilibrium phase transitions in cellular automata, and more generally, in particle systems. The model we exhibited counts among the simplest models that display DP or DP_2 phase transitions. To that respect, they can be used as a good basis for exploring second order phase transitions by analytical means or by numerical simulations.

A first step for an in depth understanding of asynchronous cellular automata is to make a "reduction" between different rules that were studied here, *i.e.,* to make a correspondence showing that if one of them has such a phase transition, then the others behave similarly. Another step would be to extend such a reduction to other well-studied systems such as synchronising systems [17] or Domany-Kinzel probabilistic CA [8]. This task would be interesting since synchronous ECA have two types of phase transition: the transition form the active to inactive phase can be obtained either by decreasing or by increasing the control parameter. It is to our knowledge the first examples where this two-way transitions are observed.

Another possibility for uniting the study of all the DP ECA is to consider a rule with synchrony rate as a point in the space of *probabilistic* cellular automata. In this space, which is homeomorphic to $\mathbb{R}^8$, it would be interesting to determine the frontiers where such phase transitions occur, in particular to know whether the DP phase transition can be explained in terms of crossing of a hypersurface [7].

The challenge is now to find examples of similar phase transitions in nature. For example, we could ask whether similar mechanisms could explain the trigger of the self-organisation phase in cellular societies [10, 2]. In an engineering context, the fact that a distributed system may change its behaviour in a totally decentralised way is also promising. In the case were brutal changes of dynamics are desired, exploiting phase transitions could allow a system to change its behaviour without any centralisation of information, for example for performing a self-diagnosis.

REFERENCES

[1] Pierre Berg, Yves Pomeau, and Monique Dubois. (1994). *Des rythmes au chaos*. Odile Jacob.

[2] Hugues Berry. (2003). Nonequilibrium phase transition in a self-activated biological network. *Physical Review E*, 67:031907.

[3] Hugues Bersini and Vincent Detours. (July 1994). Asynchrony induces stability in cellular automata based models. In Brooks, R. A, Maes, and Pattie, editors, *Proceedings of the 4th International Workshop on the Synthesis and Simulation of Living Systems* $ArtificialLifeIV$, pages 382–387. MIT Press.

[4] Hendrik J. Blok and Birger Bergersen. (1999). Synchronous versus asynchronous updating in the "game of life". *Physical Review E*, 59:3876–9.

[5] S.R. Broadbent and J.M. Hammersley. (1957). Percolation processes I. crystals and mazes. *Proceedings of the Cambridge Philosophical Society*, 53(3):629–641.

[6] Buvel, R.L. and Ingerson, T.E. (1984). Structure in asynchronous cellular automata. *Physica D*, 1:59–68.

[7] H. Chaté and P. Manneville. (1988). Spatio-temporal intermittency in coupled map lattices. *Physica D*, 32:409–422.

[8] Eytan Domany and Wolfgang Kinzel. (1984). Equivalence of cellular automata to ising models and directed percolation. *Physical Review Letters*, 53:311–314.

[9] Nazim Fatès. Fiatlux CA simulator in Java. See `http://nazim.fates.free.fr` for downloading.

[10] Nazim Fatès. (2003). Experimental study of elementary cellular automata dynamics using the density parameter. In *Discrete models for complex systems, DMCS '03 (Lyon)*, Discrete Mathematics Theoretical Computer Science Proceedings, AB, pages 155–165. Assoc. Discrete Math. Theor. Comput. Sci., Nancy.

[11] Nazim Fatès. (2004). *Robustesse de la dynamique des systèmes discrets : le cas de l'asynchronisme dans les automates cellulaires*. PhD thesis, 'Ecole normale supérieure de Lyon.

[12] Nazim Fatès. (2006). Directed percolation phenomena in asynchronous elementary cellular automata. In Samira El Yacoubi, Bastien Chopard, and Stephania Bandini, editors, *7th International Conference on Cellular Automata for Research and Industry Proceedings*, volume 4173 of *LNCS*, pages 667–675. Springer.

[13] Nazim Fatès and Michel Morvan. (2005). An experimental study of robustness to asynchronism for elementary cellular automata. *Complex Systems*, 16:1–27.

[14] Nazim Fatès, Michel Morvan, Nicolas Schabanel, and Eric Thierry. (2006). Fully asynchronous behavior of double-quiescent elementary cellular automata. *Theoretical Computer Science*, 362:1–16.

[15] Nazim Fatès, Damien Regnault, Nicolas Schabanel, and Eric Thierry. (2006). Asynchronous behavior of double-quiescent elementary cellular automata. In José R. Correa, Alejandro Hevia, and Marcos A. Kiwi, editors, *LATIN 2006 Proceedings*, volume 3887 of *Lecture Notes in Computer Science*, pages 455–466. Springer.

[16] Peter Gács. (2003). Deterministic computations whose history is independent of the order of asynchronous updating. `http://arXiv.org/abs/cs/0101026`.

[17] Peter Grassberger. (March 1999). Synchronization of coupled systems with spatiotemporal chaos. *Physical Review E*, 59(3):R2520.

[18] Haye Hinrichsen. (2000). Nonequilibrium critical phenomena and phase transitions into absorbing states. *Advances in Physics*, 49:815–958.

[19] Iwan Jensen. (1991). Universality class of a one-dimensional cellular automaton. *Physical Review A*, 43(6):3187–3189.

[20] Iwan Jensen. (1994). Critical exponents for branching annihilating random walks with an even number of offspring. *Pysical Review E*, 50(55):3623.

[21] Wolfgang Kinzel. (1983). Directed percolation. In R. Zallen G. Deutscher and J. Adler, editors, *Percolation Structures and Processes*, page 425. Adam Hilger Pub. Co., Bristol.

[22] Pierre-Yves Louis. (September 2002). *Automates Cellulaires Probabilistes : mesures stationnaires, mesures de Gibbs associées et ergodicité*. PhD thesis, Université des Sciences et Technologies de Lille.

[23] Sven Lübeck. (2004). Universal scaling behavior of non-equilibrium phase transitions. *International Journal of Modern Physics B*, 18(31-32):3977–4118.

[24] Edward F. Moore. (1962). Machine models of self-reproduction. *Proceedings of Symposia in Applied Mathematics*, 14:17–33. (Reprinted in Essays on Cellular Automata, A.W. Burks (ed.), University of Illinois Press, 1970).

[25] Luis G. Morelli and Damian H. Zanette. (July 1998). Synchronization of stochastically coupled cellular automata. *Physical Review E*, pages R8–R11.

[26] Géza Ódor, Nino Boccara, and György Szabó. (1993). Phase pransition study of a one-dimensional probabilistic site-exchange cellular automaton. *Physical Review E*, 48(4):3168–3171.

[27] Géza Ódor and Attila Szolnoki. (1996). Directed-percolation conjecture for cellular automata. *Physical Review E*, 53(3):2231–2238.

[28] Gza Ódor. (2004). Universality classes in nonequilibrium systems. *Reviews of modern physics*, 76.

[29] Andrea Roli and Franco Zambonelli. (2002). Emergence of macro spatial structures in dissipative cellular automata. In *Proc. of ACRI2002: Fifth International Conference on Cellular Automata for Research and Industry*, volume 2493 of *Lecture Notes in Computer Science*, pages 144–155. Springer.

[30] Jean-Baptiste Rouquier. (2006). Coalescing cellular automata. In ICCS'06 *Proceedings – LNCS 3993*, pages 321–328.

[31] Birgitt Schönfisch and André de Roos. (1999). Synchronous and asynchronous updating in cellular automata. *BioSystems*, 51:123–143.

8 ACKNOWLEDGEMENTS

The author expresses his acknowledgements to anonymous referees as well as H. Berry, A. Boumaza, A. Dutech, N. Paul and B. Scherrer for their careful reading of the manuscript.